https://doi.org/10.5194/hess-2023-256
Preprint. Discussion started: 2 November 2023

Hydrology and Earth System Sciences
Open Access
Discussions

Simulation of spatially distributed sources, transport, and transformation of nitrogen from fertilization and septic system in an exurban watershed

Ruoyu Zhang[1], Lawrence E Band[1,2], Peter M Groffman[3,4], Amanda K Suchy[3,5], Jonathan M Duncan[6], Arthur J Gold[7]

[1]Department of Environmental Sciences, University of Virginia, Charlottesville, 22904, USA
[2]Department of Civil and Environmental Engineering, University of Virginia, Charlottesville, 22904, USA
[3]Environmental Sciences Initiative, Advanced Science Research Center at The Graduate Center, City University of New York, New York, 10031, USA
[4]Cary Institute of Ecosystem Studies, Millbrook, 12545, USA
[5]Institute for Great Lakes Research and Biology Department, Central Michigan University, Mount Pleasant, 48858, USA
[6]Department of Ecosystem Science and Management, Pennsylvania State University, University Park, 16802, USA
[7]Department of Natural Resources Science, University of Rhode Island, Kingston, 02881, USA

Correspondence to: Ruoyu Zhang (rz3jr@virginia.edu)

Abstract. Excess export of reactive nitrogen in the form of nitrate (NO_3^-) export from exurban watersheds is a major source of water quality degradation and threatens the health of downstream and coastal waterbodies. Ecosystem restoration and best management practices (BMPs) can be introduced to reduce in-stream NO_3^- loads by promoting vegetation uptake and denitrification on uplands. However, accurately evaluating the effectiveness of these practices and setting regulations for nitrogen inputs requires an understanding of how human sources of nitrogen interact with ecohydrological systems. We evaluated how the spatial and temporal distribution of nitrogen sources, and the transport and transformation processes along hydrologic flowpaths control nitrogen cycling, export, and the development of "hot spots" of nitrogen flux in suburban ecosystems. We chose a well-monitored exurban watershed, Baisman Run in Baltimore County, Maryland, USA, to evaluate patterns of in-stream NO_3^- concentrations and upland nitrogen-related processes in response to three common activities: irrigation, fertilization, and on-site sanitary wastewater disposal (septic systems). We augmented a distributed ecohydrological model, RHESSys, with estimates of these additional loads to improve prediction and understanding of the factors generating both upland nitrogen cycling and stream NO_3^- concentrations. The augmented model predicted streamflow-weighted NO_3^- concentrations of 1.37 mg NO_3^--N/L, compared to observed 1.44 mg NO_3^--N/L, while the model predicted concentrations of 0.28 mg NO_3^--N /L without the additional loads from human activities from water year 2013 to 2017. Estimated denitrification rates in grass lawns, a dominant land cover in suburban landscapes, were in the range of measured values. The highest predicted denitrification rates were downslope of lawn and septic locations in a constructed wetland, and at a sediment accumulation zone at the base of a gully receiving street drainage. These locations illustrate the development of hot spots for nitrogen cycling and export in both planned and "accidental" retention features. Appropriate siting of best BMPs and the identification of spontaneously developed nutrient hot spots should be pursued to retain nutrients and improve water quality.

1 Introduction

Nitrogen (N) and carbon (C) are fundamental elements for ecosystem functions and are influenced by multiple factors including climate (Campo & Merino, 2016; Crowther et al., 2016), moisture and other soil properties (Pastor & Post, 1986; Wang et al., 2020), plant and microbial community composition (Chen et al., 2003), and human activities (Galloway et al., 2008). They are also influenced by the state and pattern of drainage flowpaths as different forms of C and N are mixed and transported to distinct edaphic conditions, potentially forming "hot spots" (McClain et al., 2003) that have a disproportionate influence on landscape and watershed scale biogeochemical cycling functions. Understanding mechanisms of C and N cycling and interactions with hydrologic processes is necessary to design and implement efficient ecosystem service restoration strategies. In urban, suburban and exurban ecosystems, human disturbance to biogeochemical cycling has led to air and water quality degradation and created a need for best management practices (BMPs) to improve local and downstream water quality, increase C and N retention, and promote ecosystem resilience to prepare for extreme weather events with changing climate. Therefore, gaining a comprehensive understanding of the ecohydrological behaviors and interactions between ecosystems and human activities can lay the foundation for effectively mitigating these environmental issues through well-conceived and sustainable management practices.

Several ecohydrological models have been developed to understand and quantify individual or integrated ecohydrological processes in unmanaged to highly managed ecosystems. Semi-distributed hydrologic models, such as the Storm Water Management Model (Rossman, 2010b) and the Soil Water Assessment Tool (Arnold et al., 1998), are widely used in studies of urban and mixed land use watersheds (Jayasooriya & Ng, 2014; Koltsida et al., 2023; Lee et al., 2018; Rossman, 2010a; Samimi et al., 2020). These models simulate water balance based on subcatchment units with similar land cover and soil. Runoff from each subunit is based on curve numbers or infiltration excess, and are independently added to streamflow. However, these models lack hillslope water and nutrient mixing along hydrologic flowpaths that are important to simulate the formation of biogeochemical hot spots, and the potential uptake and retention of water and nutrients within hillslopes. Patch-based ecosystem models, such as Biome-BGC (Hidy et al., 2016; Running & Gower, 1991), DAYCENT (Del Grosso et al., 2005) or the Community Land Model (Lawrence et al., 2019; Oleson et al., 2008) are designed to capture 1-dimensional patch-level water balance and biogeochemical processes affecting C and N, but also lack lateral drainage through topographically mediated flowpaths. Ignoring lateral redistribution of water and nutrients within terrestrial ecosystems may generate significant bias in estimating key hydrologic and biogeochemical processes (Band et al., 1993; Fan et al., 2019).

Fully distributed hydrology models, such as MIKE-SHE (Abbott et al., 1986a, 1986b), ParFlow (Maxwell, 2013), RTM-PiHM (Bao et al., 2017; Zhi et al., 2022) and RHESSys (Tague & Band, 2004) simulate coupled surface and subsurface hydrological processes with detailed topographic and soils information to generate distributed surface runoff, recharge, soil moisture, evapotranspiration (ET), and other ecohydrological variables. Lateral surface and subsurface drainage redistribute precipitation, resulting in gradients of water availability within a watershed from ridge to riparian areas. These models include modules for biogeochemical reaction and transport processes, which can interact with the transport and storage patterns of soil water and provide high-resolution output for each location within a watershed.

Additional inputs of water (e.g., lawn irrigation and septic effluent), C (e.g., mulch, lawn amendments) and N (e.g., septic system, lawn and garden fertilization, sanitary sewer leakage) occur on discrete land segments and can be significant or even dominant components of watershed mass budgets. Lawn fertilization can contribute more than half of the total N input in urban watersheds, even if it is only applied to 20 – 30% of the landscape (Band et al. 2005; Groffman et al., 2004; Hobbie et al. 2017). Atmospheric deposition and septic system wastewater N can comprise similar input amounts at the watershed scale, but septic input is concentrated over only 1-2% of the landscape, with a large, localized volume of wastewater sufficient to result in groundwater mounding and effluent plumes extending towards local streams (Cui et al., 2016). The concentrated inputs over limited areas by septic inputs and lawn fertilization with or without irrigation creates delivery or retention patterns of N hot spots that provide opportunities for targeting N mitigation strategies (Groffman et al., 2023).

A spatially explicit framework that simulates interactions between C, N, vegetation, water, and human activities has important advantages to understand and manage non-point source pollutants and hot spots in urban watersheds (Bernhardt et al., 2017; Groffman et al., 2009). This framework should have the flexibility for users to design and evaluate the effectiveness of potential management scenarios (e.g., reforestation, green infrastructure, etc.) and regulations at the scale of human activity. Landscape management and treatment at these scales occur as part of residential, commercial, and institutional use spaces, and may require direct involvement of residents and other stakeholders. Therefore, the ability to represent processes at the scale of human perception can also provide information useful for decision making and community involvement. High-resolution simulations and visualization of spatially explicit water, nutrient cycling, and transport can facilitate understanding and communication of how human activity can alter terrestrial and aquatic ecosystem functions in urban ecosystems and contribute to participatory planning.

The Regional Hydro-Ecological Simulator System (RHESSys, Tague & Band, 2004) is an ecohydrological model that simulates spatially distributed mass balances of water, C, and N of a watershed including hydrologic and biogeochemical stores and cycling. The hydrologic component in RHESSys routes water and solutes based on topographic and infrastructure surface water flowpaths, and two-dimensional subsurface flow based on shallow groundwater gradients. Biogeochemical process rates are then estimated with modules modified from Biome-BGC (Running & Hunt, 1993) and $\mathrm{CENTURY_{NGAS}}$ (Parton et al., 1996) and subsequent models. RHESSys is therefore capable of estimating spatiotemporal patterns of soil moisture, lateral redistribution, and evapotranspiration. By adding discrete human inputs of water and N, the distributed soil water content and groundwater levels interact with biogeochemical processes, canopy evapotranspiration, and other ecosystem processes in spatially explicit manners. Therefore, RHESSys has the flexibility to simulate at resolutions commensurate with human perception of the landscape, facilitating assessment of small-scale human activity and modification to land cover and infrastructure.

In this study, we developed and used an augmented version of RHESSys to investigate the spatial and temporal distribution of hydrologic and biogeochemical N cycling and export in a low-density suburban (exurban) watershed. Baisman Run (BARN)

https://doi.org/10.5194/hess-2023-256
Preprint. Discussion started: 2 November 2023

Hydrology and Earth System Sciences
Discussions

is in a suburban area of Baltimore County, with all households using septic systems and well water. We ran simulations with and without human additions of water and N and compared model results to field observations for streamflow, water chemistry, and soil N cycling processes to answer the following research questions:

1) What are the individual and interacting contributions of different watershed N sources to streamwater N export?

2) How do the spatially nested patterns of water and N inputs from human activities alter spatial patterns of key ecohydrological processes including N retention, evapotranspiration, soil and groundwater levels and flows?

3) What are the emergent patterns of N cycling and retention, including hot spots at sites receiving direct additional N and downslope, offsite locations receiving transported N?

2 Method

2.1 Study Area

Our study watershed (Fig. 1), Baisman Run (BARN), is in Baltimore County, MD, outside of the urban sanitary sewer service boundary. The 3.8 km^2 watershed is in the Piedmont physiographic province with a rolling, locally steep landscape. Mean elevation is 170.5 m, with average slope 7.8°. Meteorological records from 2000 to 2018 were integrated from Baltimore/Washington International Airport (BWI) weather station and a local rain gage adjacent to BARN at the Oregon Park operated by the Baltimore Ecosystem Study (BES). The records have mean annual maximum and minimum temperatures of 18.9 °C and 7.9 °C respectively, and mean annual precipitation of 1,024 mm. The discharge and gage height records of BARN have been monitored by USGS (Gage ID: 01583580) since 1999.

Soils in BARN range from silt clay loam to silt loam in the riparian areas to sandy loam on steeper slopes. Forested areas are dominated by approximately 100-year-old *Quercus spp*. (oaks) and *Carya spp.* (hickory). The entire watershed is underlain by the medium- to coarse-grained micaceous schist of the Loch Raven Formation, overlain by a weathered saprolite. The saprolite thickness is highest on ridges (up to 20m), thins (< 1 m) with some bedrock outcrops at steep midslope positions, and is 1–2 m in bottomland locations (Cleaves et al. 1970; St. Clair et al., 2015). Hydraulic conductivities of soils generally decrease with depth but may locally increase into the saprolite. The saprolite may store substantial amounts of moisture, and is drained through underlying bedrock fractures through a set of emergent springs on the valley sidewall-riparian area transition, providing a fairly steady baseflow (Putnam, 2018). Dominant land cover includes forest and lawns, covering 81.5% and 14.5% of the watershed, respectively. Impervious areas cover 4.0% of the watershed, including roofs of single-family houses, driveways and roads. Lawns are located in front and backyards of households in headwater areas of BARN. Two natural gas supply lines cut through the watershed, creating two strips of herbaceous land.

BARN is a useful watershed for examining the interactions between human activities and watershed ecohydrological response, as the sources and disposal of domestic water are on-site without external piped inputs and outputs. In this exurban watershed all households use groundwater wells for water supply and on-site septic systems to process wastewater. Lawn and garden

https://doi.org/10.5194/hess-2023-256
Preprint. Discussion started: 2 November 2023

Hydrology and Earth System Sciences
Discussions

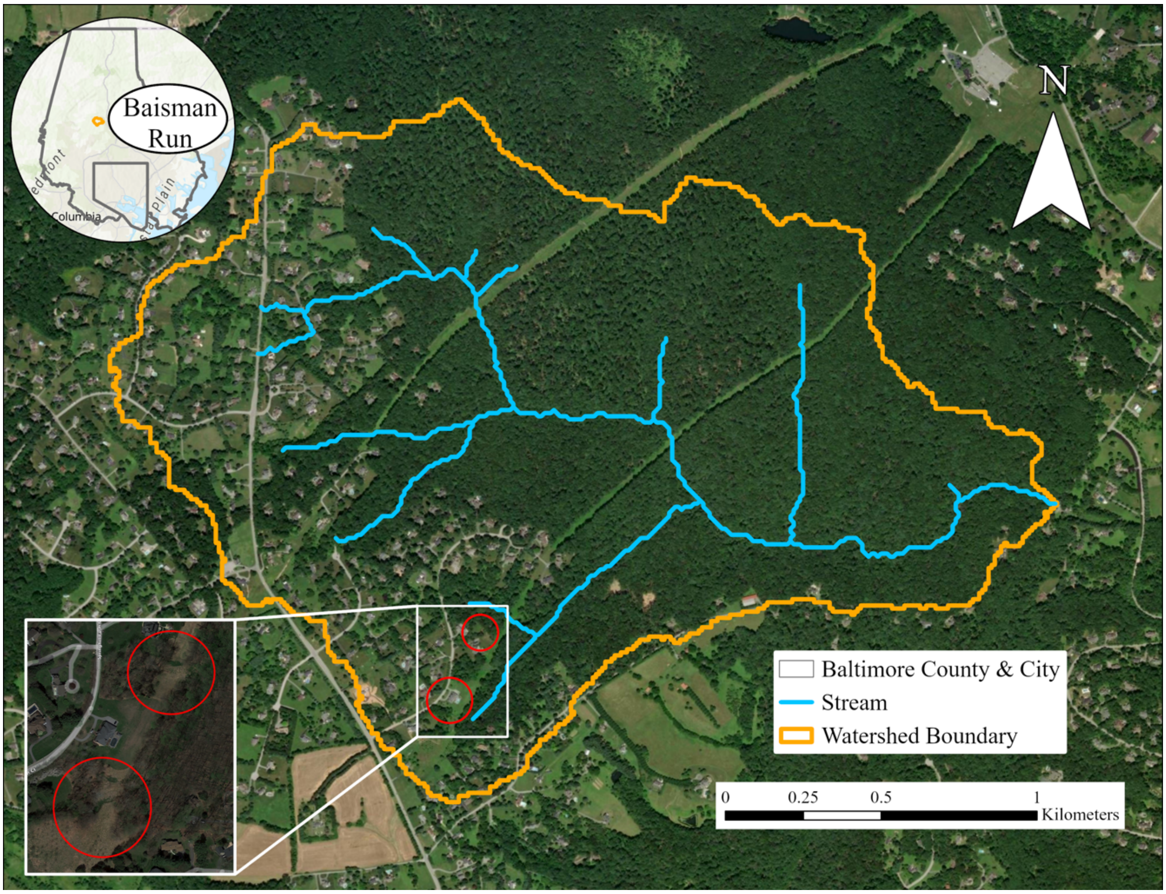

Figure 1. Study watershed Baisman Run (BARN) in suburban Baltimore County, Maryland. The white box highlights two "hot spots": A sediment accumulation zone (upper circle) receiving drainage from roads and a constructed wetland (lower circle). These areas have a high capacity to prevent N from upland residential areas from being transported to streams. Base map (World Imagery) sources: Esri, DigitalGlobe, GeoEye, i-cubed, USDA FSA, USGS, AEX, Getmapping, Aerogrid, IGN, IGP, swisstopo, and the GIS User Community.

fertilization is another major source of N input in BARN (Law et al., 2004). Septic and fertilization N and water additions are localized on lawns and septic drain fields near houses in the BARN headwaters. Irrigation and septic effluent are derived from well water, pumping deep groundwater to shallow soils.

The availability of several previously collected data sets allowed us to compare simulation results to field observations. Rich ecohydrological observations and lawn management surveys (Fraser et al., 2013; Law et al., 2004) from the BES are available as are weekly water chemistry concentration data at the BARN USGS gage since 1998 (Castiblanco et al. 2023). In addition, a fully forested subcatchment of BARN, Pond Branch (POBR), is also monitored weekly by the BES and USGS (Gauge ID: 01583570). POBR serves as a forest control site without human water and nutrient additions. Finally, we have previously measured N stores and cycling rates, including lawn soil NO_3^- content and denitrification rates in BARN (Suchy et al., 2023), sites on the campus of the University of Maryland Baltimore County (Raciti et al., 2011), and other sites in the region (Groffman et al., 2009). Atmospheric N deposition was estimated as 11 kg N/ha/year.

2.2 RHESSys setup and calibration

Our study period makes use of observed and simulated watershed processes from water year 2013 to 2017 (i.e., Oct. 1, 2012 to Sep. 30 2017), with a 30-year simulation spinup period to stabilize groundwater levels and C and N pools. Inspection of the spin-up storage of soil C and N showed they were asymptotic with stable C:N ratios. The watershed is delineated using 1-m digital elevation data accessed from the Maryland GIS portal (https://data.imap.maryland.gov) and r.watershed from GRASS GIS (https://grass.osgeo.org/grass82/manuals/r.watershed.html). Streams are identified when accumulated drainage areas are above 10 ha (Fig. 1), which approximates the extension of Baltimore County's hydrology lines dataset (https://opendata.baltimorecountymd.gov/datasets/hydrology-lines). Detailed land use information is derived from the 1-m high-resolution land use and land cover (LULC) data from the Chesapeake Conservancy (https://www.chesapeakeconservancy.org/conservation-innovation-center/high-resolution-data/lulc-data-project-2022). The dataset contains "roof" as a LULC class, from which we identified 249 spatially isolated clusters of roofs within BARN. Comparison with the Baltimore County parcel dataset (https://opendata.baltimorecountymd.gov) and latest Google Earth satellite data allow us to filter out detached garages and sheds and to identify the main building in each parcel. We identified 181 households, although a set of the homes are located on the watershed divide, providing some uncertainty to the effective number of septic systems. We set up RHESSys in BARN at 10-m resolution. Patches in centroids of the 181 main buildings were identified as "drain-in" patches, receiving pumped groundwater. Drain-in patches were paired with "drain-to" patches, which were designated to receive septic wastewater additions and will be discussed in detail in the next section. The riparian areas in RHESSys were defined as areas with height above nearest drainage (HAND, Nobre et al., 2011) below 1.5 meters. These areas were set to receive additional drainage from the deep groundwater system. The start and end of the growing season are hardcoded in RHESSys and vary for different vegetation species, where deciduous trees from May 5th to Oct 22nd and grass is set as a perennial, identical to parameters in Lin et al., 2015 & 2019. Sensitivity analysis of the length of the grass growing season showed negligible impacts on ecohydrological responses as temperature becomes a limiting factor.

RHESSys requires several parameters to simulate lateral and vertical water flows within soils and topography. In this study, we calibrated eight parameters (Table 1) for soil properties (i.e., lateral and vertical saturated hydraulic conductivities and their decay rates, pore size index, and air entry pressure) with initial estimates from the SSURGO soils dataset (https://data.nal.usda.gov/dataset/soil-survey-geographic-database-ssurgo) and deep groundwater features (i.e., bypass seepage from surface and shallow saturated soil, and drainage rate to stream). These original parameter values were further calibrated by multipliers listed in Table 1 against the daily USGS discharge records, and the parameter set yielding the highest Nash-Sutcliffe efficiency (NSE, Nash & Sutcliffe, 1970) was used to simulate ecohydrological processes in this study.

https://doi.org/10.5194/hess-2023-256
Preprint. Discussion started: 2 November 2023

Table 1. Calibrated multipliers for RHESSys parameters generating the highest NSE for streamflow

Sensitivity Parameter	Name	Details	Value
s	m	decay of hydraulic conductivity with depth	0.924
	K	hydraulic conductivity at the surface	0.707
	depth	soil depth	4.835
sv	m	vertical decay of hydraulic conductivity with depth	0.659
	K	hydraulic conductivity at the surface	1.601
svalt	po	pore size index	1.798
	pa	air entry pressure	0.509
gw	surf_coeff	bypass fraction to deep groundwater from surface	0.010
	gw_loss_coeff	groundwater storage/outflow parameters	0.916
	sat_coeff	bypass fraction to deep groundwater from saturation zone	0.034

2.3 Human additions of water and N

We included estimates of fertilization, onsite wastewater disposal from septic systems, and irrigation, as input to RHESSys to incorporate water and N management decisions and capture how such activities affect water and N cycling and export within the study watershed.

2.3.1 Fertilization

The lawn fertilization module in RHESSys allows users to determine the fertilization rate and when and where applications are applied to lawns. Law et al. (2004) and Fraser et al. (2013) conducted in-person household surveys in a set of neighborhoods in the Baltimore area, including BARN, and found that approximately 50% of homeowners apply fertilizer to their lawns, with a mean annual total fertilization rate ranging from 3.7 to 13.6 g N/m^2. Both surveys were conducted during significant drought conditions (2002 and 2008) when lawncare was reduced due to groundwater supply concerns. Hence, we consider the survey results to be on the lower end of actual rates. In this study, we used the intermediate lawn fertilization rate reported in Law et al. in 2004, 8.4 g N/m^2 (12.4 kg N/ha/year at watershed scale, accounting for lawns that are not fertilized), for a denser suburban site, Glyndon, in Baltimore. We assumed all lawns in BARN were fertilized three times with a 60-day interval between applications beginning April 1. This fertilization frequency is consistent with our prior household surveys and similar to results of surveys conducted in other suburban communities (Carrico et al., 2013; Martini et al., 2015). The model distributed the estimated total fertilization amount uniformly to all lawns in the watershed, at rates modulated by the proportion of lawns fertilized estimated by Law et al. (2004) and Fraser et al. (2013).

https://doi.org/10.5194/hess-2023-256
Preprint. Discussion started: 2 November 2023

Hydrology and Earth System Sciences
Discussions

In the model, applied fertilizer is stored in an independent pool of each lawn patch, and each day we assumed a fixed fraction of available nutrients in the fertilizer pool leached to other pools, of which 80% is dissolved to detention storage and 20% to soil. The daily leaching fraction (LF) is determined by the fertilization interval (FI), following Eq. (1):

$$LF = -\frac{log\ 0.1}{FI}, \tag{1}$$

In our case study, our 60-day fertilization interval results in 3.8% of nutrients in the fertilization pool transported to other pools per day and then stored, consumed by vegetation, immobilized, or further transported to groundwater and downslope. In this study, we considered fertilizer input only contains NO_3^-, following sensitivity analysis that found varying NO_3^- and NH_4^+ proportion in fertilizer had negligible impacts on model outputs. Phosphorous fertilizer, which is increasingly uncommon in many lawn fertilizer formulations, is not considered as RHESSys currently does not simulate the phosphorous cycle.

2.3.2 Septic system

All households within BARN use septic systems to disperse wastewater. Wastewater from a house is released first to septic tanks for settling, then to drain fields which are typically placed downslope of the house. Therefore, soils in specified, downslope areas receive additional water and N input from septic effluents and may become hot spots sources of NO_3^- in the watershed. Using data from prior studies, we estimated the N load from septic systems as 7.7 kg N/capita/year and water input as 110.5 m^3/capita/year (~80 gal/capita/day), resulting in a NO_3^- concentration of 70 mg N/L which is comparable to those reported by Gold et al. (1990) and Lowe et al. (2009). We set the average number of people per household as 3.3 for these single-family houses based on survey results from Law et al. (2004) and census information. Applying these water and NO_3^- loads for 181 houses in BARN results in 4,599 kg N/year (12.0 kg N/ha/year) of NO_3^- input to the watershed; The demand for septic source water (SSW_{demand}) is 110,058 m^3/year (29.2 mm/year) of water extracted from deep groundwater. Septic water and N loads are currently set to be evenly distributed every day.

Septic source water is drawn from drain-in patches (i.e., centroid patches of main buildings) and transported to storage in septic drain-to patches (Fig. 2) which are the locations of drain fields of septic systems and defined as the closest downslope lawn patches to drain-in patches. We regulated actual withdrawal of septic source water (SSW_{actual}) to not exceed the available water in groundwater storage, as in Eq. (2):

$$SSW_{actual} = min(SSW_{demand}, GW_{storage}), \tag{2}$$

where $GW_{storage}$ is available water in surface detention and deep groundwater storage of the hillslope at drain-in patches (Fig. 2). The extracted source water is added to septic drain-to patches (orange arrow in Fig. 2), where it is subject to hydrological and biogeochemical processes. Nutrients are also added to the drain-to patches' storage, depending on concentrations and quantity of source water from the groundwater of drain-in patches.

2.3.3 Irrigation

Although irrigation practices and quantities vary significantly among households, irrigation is commonly applied during the

https://doi.org/10.5194/hess-2023-256
Preprint. Discussion started: 2 November 2023

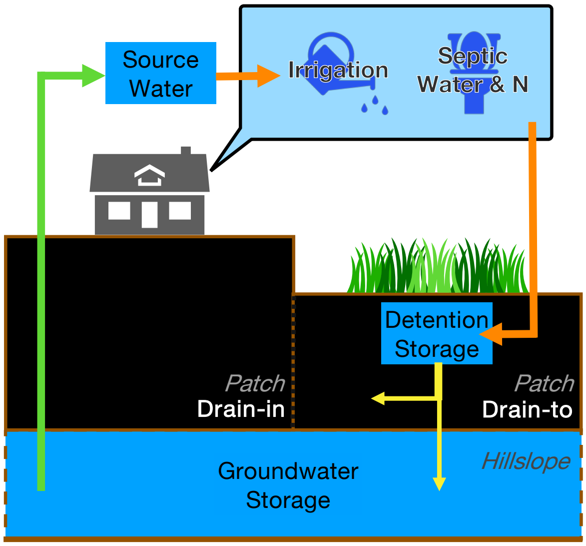

Figure 2. Groundwater extraction for irrigation and septic systems in the RHESSys model. The source water (green arrows) is extracted from groundwater storage of drain-in patches (i.e., house centroids) and redistributed to surface detention in downslope lawn patches after usage (i.e., drain-to patches, see Method) for septic and irrigation purposes (orange arrows). After redistribution of source water, infiltration (yellow arrows) to soil and percolation to hillslope groundwater would follow the original processing of RHESSys

growing season, and especially during dry and hot conditions. Therefore, we designed a mechanism to determine the total irrigation amount based on water stress of grass. Specifically, the amount of irrigation applied on lawns is determined by a water stress factor (*WSF*) in Eq. (3):

$$WSF = \frac{PET - ET}{PET}, \tag{3}$$

where PET and ET represent patch level potential and actual ET. During continuously hot and dry days, WSF would increase due to lower soil water content (lower ET) and high atmospheric demand for water (higher PET). Our model then activates the irrigation function and calculates the demand of irrigation for patches modulated by water shortage. This function effectively modulates soil water conditions by the addition of groundwater sourced irrigation.

Unlike the septic source water (SSW_{demand}) which is fixed each day, the daily demand for irrigation source water (ISW_{demand}) in Eq. (4) for a lawn patch is further controlled by the water stress factor as:

$$ISW_{demand} = IR_{max} \cdot WSF \cdot lawn\%, \tag{4}$$

where IR_{max} is the user-defined maximum daily irrigation rate, WSF is the water stress factor in Eq. (3), and $lawn\%$ is the fraction of grass in an irrigated patch. We defined the maximum irrigation rate (IR_{max}) in BARN as 4 mm/day in the current model, which can be modified based on the local practices or for sensitivity analysis. Like septic source water, withdrawal of irrigation source water cannot exceed available water in groundwater storage. The actual irrigation source water is calculated

https://doi.org/10.5194/hess-2023-256
Preprint. Discussion started: 2 November 2023

Table 2. Scenarios evaluated in BARN and corresponding combinations of augmented RHESSys features

Scenario Name	Irrigation	Fertilization	Septic Processes
None	✓		
Fertilization Only	✓	✓	
Septic Only	✓		✓
Both	✓	✓	✓

following the same rule in Eq. 2. The irrigation amount is pumped from deep groundwater storage to drain-in patches (i.e., centroids of houses, Fig. 2) to water lawns around houses. Irrigated lawns are limited to 50 m from houses, covering 33.7 ha (60.6%) out of 55.7 ha of lawns in BARN, a proportion consistent with survey results.

2.4 Scenarios and N hot spots

We focus on evaluating changes in NO_3^- dynamics in stream and upland areas when additional NO_3^- is added from fertilization and/or septic systems, which resulted in four scenarios (Table 2) – *none* (no fertilization or septic inputs), *fertilization only*, *septic only*, and *both* (fertilization and septic inputs) – for our study watershed. Irrigation is activated in all scenarios, including our reference control scenario "*none*" to emphasize NO_3^- dynamics without residential N inputs. Scenario *both* receives a total of 35 kg N/ha/year of N input, with 11 (31.4%), 12 (34.3%), and 12 (34.3%) kg N/ha/year from atmospheric deposition, fertilization, and septic effluents, respectively, expressed at the watershed level. We resampled the daily simulated NO_3^- concentration from RHESSys to weekly averages for comparison with the sampled weekly water chemistry from BES for BARN.

We further evaluated changes in ecohydrological processes at potential on-site hot spots (e.g., residential lawns and septic drainage fields) receiving direct human water and N inputs as well as off-site potential hot spots located in downslope areas that receive human water and N inputs added upslope (e.g., riparian areas and wetlands). Lawns are identified as patches with more than 50% of grass, and downstream forests are patches with more than 50% of forest downslope of residential area of BARN. One off-site location is a constructed wetland (upper red circle in Fig. 1), while is a spontaneously developed "accidental wetland" (Palta et al., 2017) in an area receiving road drainage and gully sedimentation, and is referred to as a "sedimentation accumulation zone" (lower red circle in Fig. 1).

https://doi.org/10.5194/hess-2023-256
Preprint. Discussion started: 2 November 2023

Hydrology and Earth System Sciences
Discussions

3 Results

3.1 Ecohydrological responses

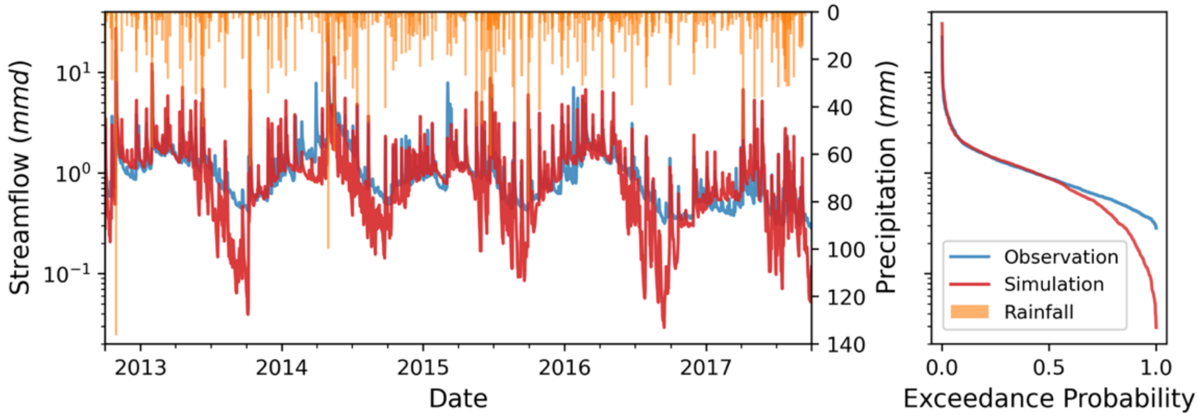

Figure 3. Comparison of streamflow time series (left) and duration curve (right, share the same y-axis of streamflow in the left figure) between USGS (blue) observations and RHESSys simulations (red) with irrigation, fertilization, and septic components i.e., scenario both

Calibration of streamflow simulations (Fig. 3) with irrigation, fertilization and septic input (scenario *both*) produced a maximum Nash-Sutcliffe value of 0.70 from water year 2013 to 2017 (Oct 1st, 2012 to Sep 30th, 2017) with calibrated parameter values listed in Table 1. The mean of simulated streamflow was 1.13 mm/day, which is slightly lower than the 1.16 mm/day mean observed runoff at the USGS gage. Our model tended to underestimate the lowest flows, with mean simulated growing season (from May to September) streamflow of 0.90 mm/day which is 0.19 mm/day lower than the 1.08 mm/day USGS records. Mean streamflow was decreased by only 0.01 mm/day by adding septic processes as this addition increased ET during the growing season (comparing to scenario *none,* Fig. 4 - upper). The increase in ET was associated with an increase in net photosynthetic rates during the growing season of 0.01 g C/m^2 (comparing scenario *none*, Fig. 4 - lower), averaged at the watershed scale. No change of streamflow or ET (< 0.01 mm/day) was found when only fertilization was activated.

3.2 Improved prediction of NO3– export

Turning fertilization and septic processes on and off in the model produced variation in in-stream NO_3^- concentration and load simulations (Fig. 5). In our 5-year study period, the mean flow-weighted NO_3^- concentrations for scenarios *none*, *septic only, fertilization only, and both* were 0.28, 0.73, 0.83, and 1.37 mg NO_3^--N/L, respectively. The mean streamflow-weighted long-term observed concentration at the BARN USGS gauge was 1.44 mg NO_3^--N/L. Thus, the simulated mean NO_3^- concentration considering both fertilization and septic loads was only 0.1 mg NO_3^--N/L (-7%) lower. At seasonal scales (Table 3), the mean simulated flow-weighted NO_3^- concentrations of scenario *both* in spring and fall were similar to the BES weekly records,

https://doi.org/10.5194/hess-2023-256
Preprint. Discussion started: 2 November 2023

Hydrology and Earth System Sciences
Discussions

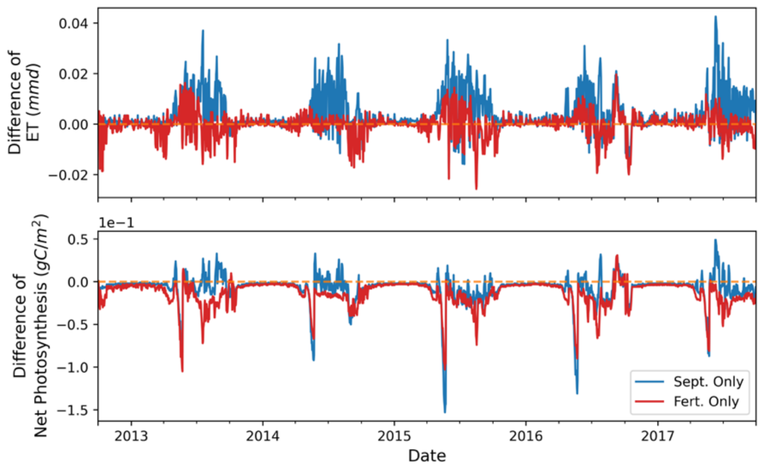

Figure 4. Difference of ET (upper) and net photosynthesis (lower) after adding septic or fertilization processes into RHESSys, i.e., comarping with the baseline of "none" scenario

higher by 0.01 (+0.8%) and 0.05 (+3.5%) mg NO_3^--N/L, respectively. In summer and winter, the simulations were lower by -0.29 (-19.0%) and -0.18 (-10.6%) mg NO_3^--N/L, respectively.

Table 3. Mean daily NO3– concentration (mg N/L, flow-weighted) and load (kg N/ha/year) for each season and the entire study period from BES weekly records (all letters capitalized, BARN and POBR) and RHESSys simulations (first letter capitalized, Both, Fert. only, Sept. only, and None) from water year 2013 to 2017

	Season	Scenario					
		BARN	**Both**	**Fert. only**	**Sept. only**	**POBR**	**None**
Flow-weighted Concentration	**Spring**	1.26	1.27	0.73	0.67	0.02	0.24
	Summer	1.53	1.24	0.76	0.63	0.05	0.25
	Fall	1.44	1.49	0.94	0.8	0.04	0.34
	Winter	1.7	1.52	0.92	0.81	0.01	0.32
	Mean	1.44	1.37	0.83	0.73	0.03	0.28
Load	**Spring**	9.95	7.54	4.34	4.00	0.01	1.40
	Summer	5.35	3.56	2.21	1.80	0.02	0.72
	Fall	4.29	3.93	2.52	2.10	0.01	0.92
	Winter	7.62	7.54	4.57	4.04	0.01	1.59
	Mean	6.80	5.64	3.42	2.99	0.01	1.16

Hydrology and Earth System Sciences
Discussions

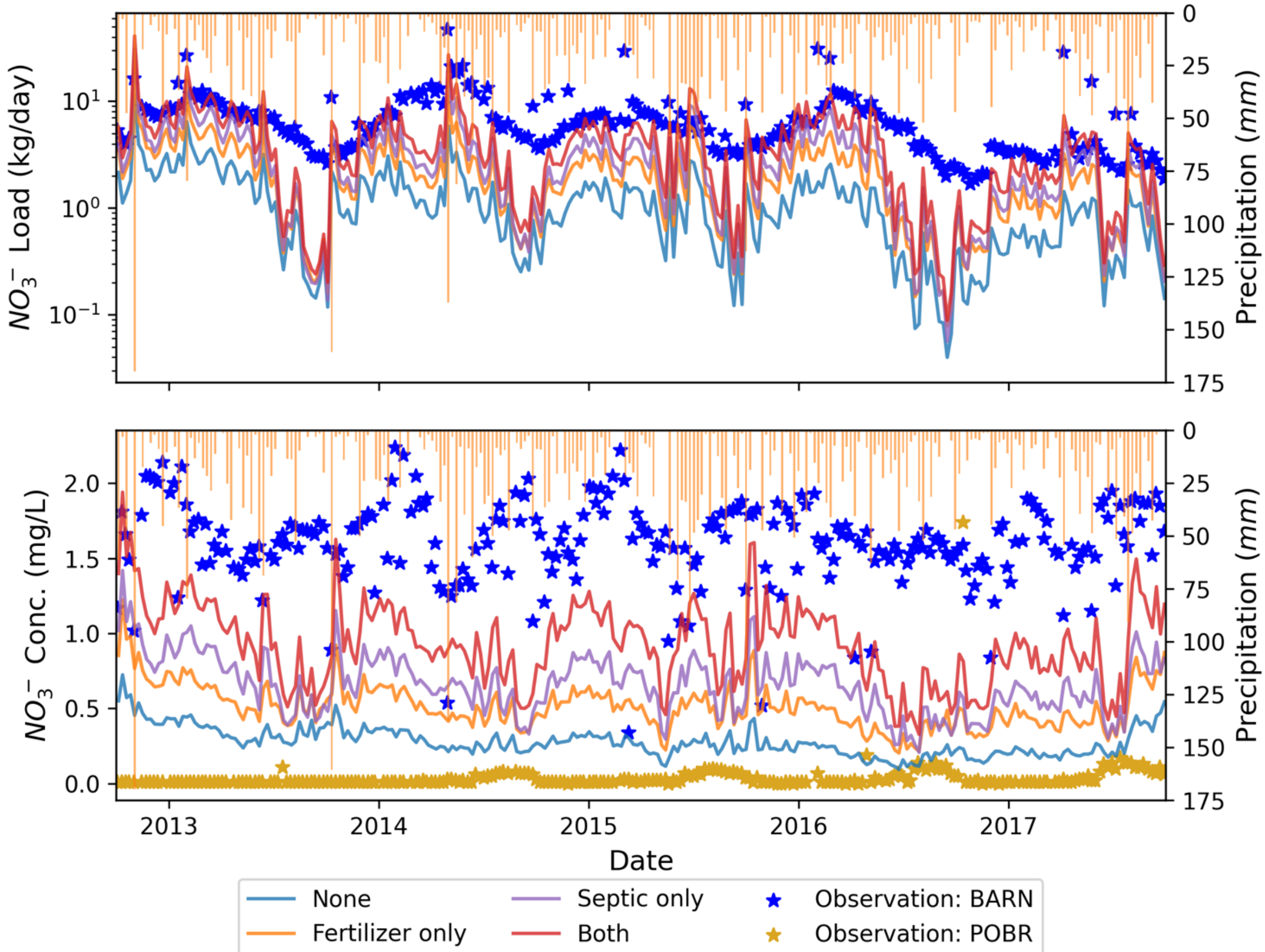

Figure 5. Mean weekly NO_3^- load (upper) and concentration (lower) from RHESSys scenarios none, fertilization only, septic only, and both fertilization and septic processes, and BES weekly NO_3^- concentration records from water year 2013 to 2017. Fertilization rate was 12.4 kg NO_3^--N/ha/year. Observed BARN load records are calculated using BES concentration and USGS discharge records. POBR loads were too small to be included

In-stream NO_3^- load (Fig. 5) followed a similar trend as concentration, but the bias was reduced substantially from scenario *none* to *both* when fertilizer and septic loads were included. Scenario *both* underestimated NO_3^- load in all seasons (by -2.41 (-24.3%), -1.79 (-33.5%), -0.36 (-8.4%), and -0.09 (-1.1%) kg NO_3^--N/ha/year in spring, summer, fall, and winter, respectively) compared to the load records calculated from BES concentration and USGS discharge observations (Table 3). The differences were due to lower simulations than observed discharges (Fig. 3). Lastly, the NO_3^- retention rate (i.e., % of N input not exported in streamflow) varied across different scenarios ranging from a high of 89% in scenario *none* (atmospheric deposition only) to

https://doi.org/10.5194/hess-2023-256
Preprint. Discussion started: 2 November 2023

Hydrology and Earth System Sciences
Open Access
EGU
Discussions

a low of 84% in scenario *both*. In scenario *septic only*, retention rate was 87%, and in scenario *fertilization only*, retention was 85%.

3.3 Ecohydrological and biogeochemical responses at hot spots

In our simulations, fertilizer is slowly released to soil and surface detention and transported downslope. This transport is augmented by irrigation and septic fields. As a result, water and NO_3^- are redistributed through other patches along subsurface hydrological flowpaths, providing "off-site" ecohydrological and biogeochemical responses downslope and across the whole watershed.

3.3.1 Soil moisture and ET

The average water table depth (Fig. 6) in scenario *none* was 4.75 m during the study period. Fertilization had negligible effects on soil moisture or water table depth compared to the base (*none*) scenario. However, septic processes decreased mean water table depth to 4.68 m (by -0.06 m, -1.3%) by groundwater mounding, which increases shallow groundwater flow to surrounding patches along connected flowpaths. Specifically in septic drainage field patches, the mean water table depth decreased to 3.64 m (-0.77 m, -17.4%) in scenarios *both* and *septic only* compared to the mean depth of 4.41 m, in scenarios *none* and *fertilization only* (Fig. 7). Setting hillslope groundwater as the only source for septic process, we found groundwater withdrawal resulted in drier conditions (i.e., increase of water table depth) in riparian areas where the mean water table depth increased to 0.22 m (+0.01 m, +4.7%) in scenarios *both* and *septic only* compared to 0.21 m depth in scenarios *none* and *fertilization only*.

The watershed-scale ET was 42.1 mm/month in scenarios *none* and *fertilization only*, and 42.2 mm/month in scenarios *septic only* and *both.* As the result of higher soil moisture levels after activating septic processes in scenario *both*, ET in lawn patches and septic drainage fields increased to (by) 39.3 (+0.2, 0.5%) and 40.7 (+7.7, 23.3%) mm/month, compared to the levels in scenarios *none* or *fertilization only*, respectively. ET in riparian areas was 54.0 and 54.1 mm/month in scenarios *none* and *septic only*; With fertilization activated in scenarios *fertilization only* and *both*, riparian ET dropped slightly by about 0.1 (-0.1%) mm/month, possibly due to the greater vegetation growth and higher ET in upland areas.

3.3.2 Denitrification

Our model suggested significant changes in denitrification after including additional NO_3^- inputs from fertilization and septic processes. The mean annual rates (Fig. 7) of denitrification at the watershed scale were 12, 12.4, and 14 kg N/ha/year in scenarios *fertilization only*, *septic only*, and *both*, respectively, increasing by 20.8%, 24.5%, and 41.3% compared to scenario *none*. There were a few locations with reduced denitrification after adding fertilization and septic processes, but only 0.57% of patches (220 out of 38,263 patches) of the watershed experienced decreases greater than 5%, with the mean rate dropping from 4.6 to 4.1 kg N/ha/year. From these patches, we further identified 19 near-stream patches (i.e., HAND < 3 m) and found that they all experienced substantial water table drops (11 mm average reduction) with septic inputs extracting groundwater.

Hydrology and Earth System Sciences
Discussions

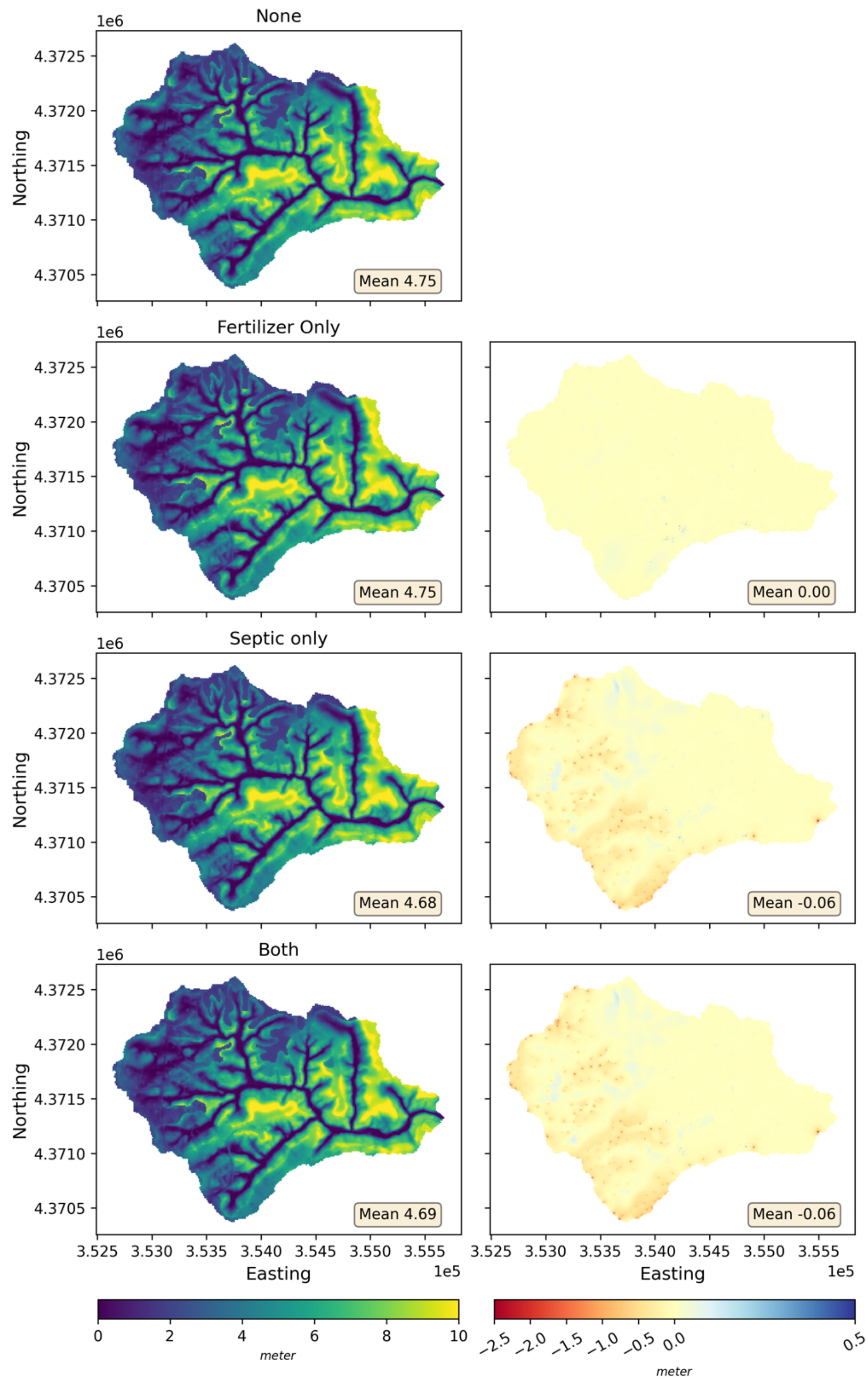

Figure 6. Water table depth (m, left) before and after considering fertilization, septic, or both inputs (i.e., scenarios none, fertilization only, septic only, and both) and corresponding changes in depth (right). Red (green) represents shallower (deeper) water table. Irrigation is applied for all scenarios showed. Maps in NAD83 UTM 18N projection

https://doi.org/10.5194/hess-2023-256
Preprint. Discussion started: 2 November 2023

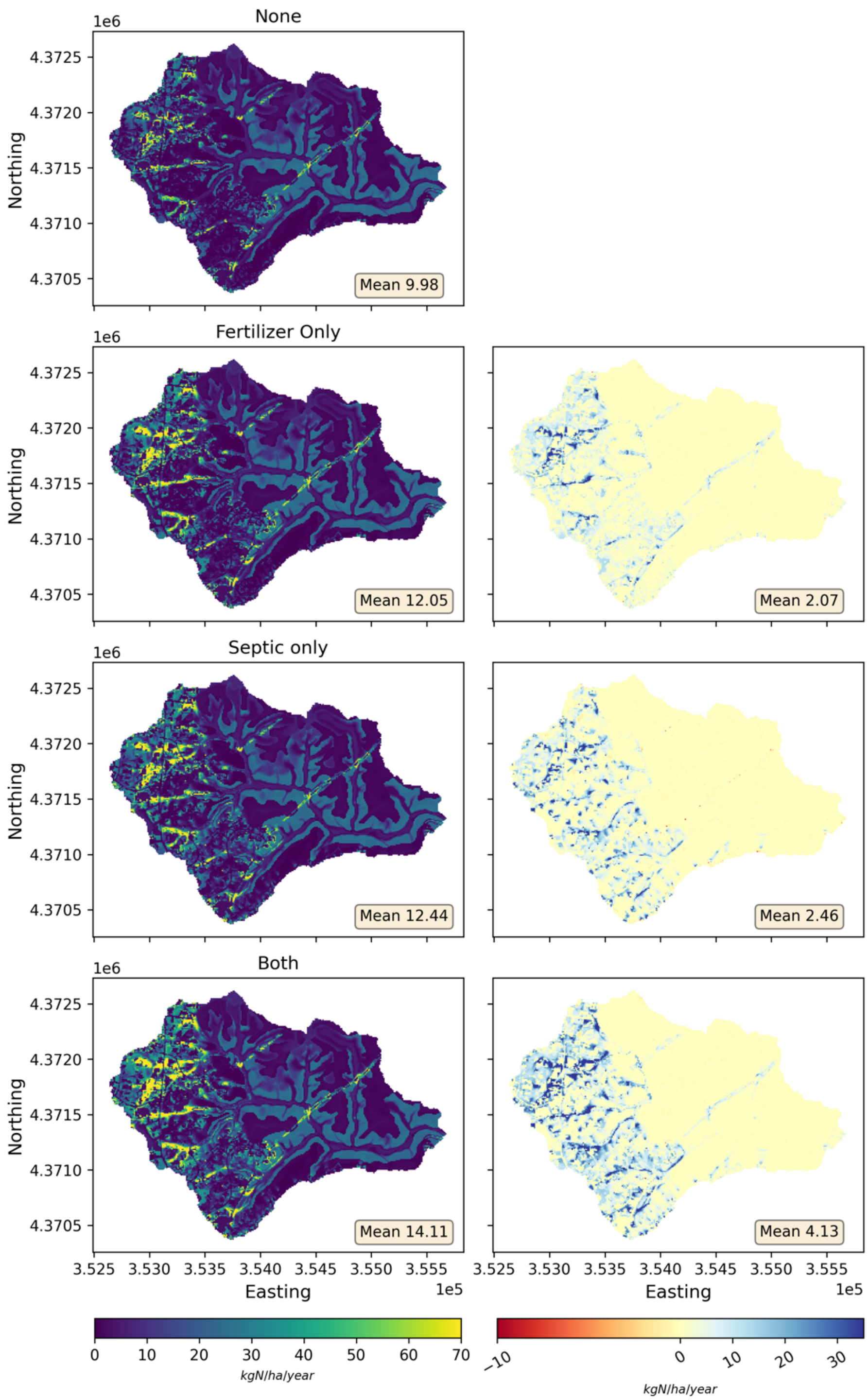

Figure 7. Denitrification (kg N/ha/year, left) after adding fertilization, septic, or both features (left) and corresponding changes in denitrification (right). Irrigation is applied for all scenarios showed. Maps in NAD83 UTM 18N projection

https://doi.org/10.5194/hess-2023-256
Preprint. Discussion started: 2 November 2023

Hydrology and Earth System Sciences
Discussions

Denitrification rates increased significantly in hot spots – lawn, septic drainage field, and riparian areas (Table 4) in response to NO_3^- inputs from fertilization and septic processes. Compared to scenario *none*, scenario *fertilization only* had higher denitrification rates than scenario *septic only* in lawns and riparian areas, except for septic drainage patches where the annual denitrification rate with only septic processes (i.e., scenario *septic only*) was almost 3-fold higher (+210%) than the reference scenario *none.* There was a 40% increase with scenario *fertilization only* compared to the reference scenario *none*.

Fertilization and septic processes added more than 20 kg N/ha/year load at the watershed level concentrated in upland residential areas. These additions increased mean denitrification rates in forest patches in and below residential areas (i.e., excluding patches in Pond Branch) by 45.2% (Table 4). The annual denitrification rates in the sedimentation accumulation zone (upper red circle in Fig. 1) showed a significant increase after activating fertilization and septic processes, reaching values of 73.8 kg N/ha/year before and 99.2 (+25.4, 34.4%) kg N/ha/year after activation. Similarly, denitrification rates in the constructed wetland (lower red circle in Fig. 1) increased from 79.3 kg N/ha/year before to 101.4 (+22.2, 28.0%) kg N/ha/year after activation.

Changes in denitrification varied among seasons (Table 4). At the watershed scale and in all hot spots, the highest rates were generally found in spring and summer, followed by fall, and lowest in winter. The greatest increases (%) in denitrification at all locations were in spring when fertilizer is applied to lawns and soil moisture is generally higher. Riparian areas had significant increases in denitrification in winter when the watershed receives sustained NO_3^- input from septic effluents.

Our modeled denitrification rates are consistent with measurements from field studies in Baltimore. Assuming 210 days (~7 months) that denitrification would occur, Raciti et al. (2011) reported a denitrification rate of 204 kg N/ha/year at 20 °C for saturated soil samples from fertilized lawns at the University of Maryland Baltimore County. At the same temperature, Suchy et al. (2023) reported a higher rate, 744 kg N/ha/year, when lawn soil samples collected from BARN were saturated. We interpolated the two rates based on the method from Raciti et al. (2011), assuming 5% storm (i.e., saturated soil) and 95% dry (i.e., low-soil-moisture) days (with a denitrification rate of 2.95 kg N/ha/year) rate in a year. The projected climate-adjusted mean denitrification rates were 13 and 40 kg N/ha/year from Raciti et al. and Suchy et al, which are very similar to estimates of annual denitrification from our simulated scenarios (Fig. 7). The 25 and 85 percentiles of annual denitrification rate for lawns in scenario *both* wee 2.94 to 31.6 kg N/ha/year, respectively, which are quite comparable with the range of empirical measurements from low to high soil moisture conditions.

4 Discussion and Conclusions

4.1 Hydrologic processes

In BARN, household water use from wells transports roughly 0.08 mm/day of water from groundwater to septic systems at the watershed level. However, the conversion of groundwater to septic usage produced only negligible changes in streamflow, while locally changing soil moisture and groundwater levels. Specifically, simulated streamflow was slightly decreased compared to the condition without septic water input. Inspecting growing season phenology, we found both ET and net

https://doi.org/10.5194/hess-2023-256
Preprint. Discussion started: 2 November 2023

Table 4. Seasonal and annual denitrification rates (kg N/ha/year) in different locations under four scenarios. Absolute and relative changes (all positive) from scenario none are reported in parentheses below denitrification rates. Rates for forest excluded Pond Branch patches where there are no fertilizer or septic inputs.

Location	Season	Scenario: None	Fertilization Only	Septic Only	Both
Lawn	Spring	13.52	18.34 (4.82, 35.7%)	16.6 (3.08, 22.7%)	20.3 (6.77, 50.1%)
	Summer	18.99	24.04 (5.05, 26.6%)	21.7 (2.71, 14.3%)	25.72 (6.73, 35.4%)
	Fall	14.27	17.44 (3.16, 22.2%)	16.6 (2.33, 16.3%)	19.11 (4.84, 33.9%)
	Winter	9.81	11.69 (1.88, 19.2%)	11.84 (2.03, 20.7%)	13.15 (3.34, 34.1%)
	Annual	14.15	17.88 (3.73, 26.4%)	16.68 (2.53, 17.9%)	19.57 (5.42, 38.3%)
Drain-to	Spring	5.62	8.21 (2.59, 46.1%)	19.83 (14.22, 253.0%)	19.84 (14.23, 253.2%)
	Summer	7.68	9.31 (1.63, 21.2%)	21.23 (13.55, 176.4%)	21.3 (13.62, 177.3%)
	Fall	6.65	7.63 (0.98, 14.7%)	20.88 (14.23, 213.8%)	20.92 (14.27, 214.5%)
	Winter	5.11	6.23 (1.12, 22.0%)	15.77 (10.66, 208.6%)	15.75 (10.64, 208.3%)
	Annual	6.27	7.85 (1.58, 25.2%)	19.43 (13.16, 210.1%)	19.45 (13.19, 210.5%)
Riparian	Spring	12	18.99 (6.99, 58.2%)	19.56 (7.56, 63.0%)	24.62 (12.62, 105.1%)
	Summer	13.53	17.99 (4.47, 33.0%)	17.65 (4.13, 30.5%)	21.41 (7.89, 58.3%)

	Fall	10.17	14.39 (4.22, 41.6%)	13.67 (3.5, 34.5%)	17.19 (7.02, 69.1%)
	Winter	8.66	13.48 (4.81, 55.6%)	13.37 (4.71, 54.4%)	16.48 (7.82, 90.3%)
	Annual	11.09	16.21 (5.12, 46.2%)	16.06 (4.97, 44.9%)	19.93 (8.84, 79.7%)
Forest	**Spring**	12.52	15.57 (3.05, 24.3%)	16.93 (4.41, 35.2%)	19.27 (6.75, 53.9%)
	Summer	9.34	11 (1.66, 17.8%)	11.3 (1.96, 21.0%)	12.91 (3.57, 38.2%)
	Fall	9.51	11.11 (1.92, 22.6%)	11.41 (1.9, 20.0%)	12.85 (3.34, 35.1%)
	Winter	8.49	10.41 (1.92, 22.6%)	11.42 (2.93, 34.4%)	12.81 (4.32, 50.9%)
	Annual	9.97	12.02 (2.06, 20.6%)	12.77 (2.8, 28.1%)	14.46 (4.49, 45.1%)
Watershed	**Spring**	11.88	14.84 (2.96, 24.9%)	15.59 (3.71, 31.2%)	17.86 (5.98, 50.4%)
	Summer	10.17	12.13 (1.96, 19.3%)	12.04 (1.87, 18.4%)	13.81 (3.64, 35.8%)
	Fall	9.69	11.34 (1.64, 16.9%)	11.46 (1.77, 18.2%)	12.89 (3.2, 33%)
	Winter	8.18	9.89 (1.71, 20.9%)	10.66 (2.48, 30.3%)	11.9 (3.71, 45.4%)
	Annual	9.98	12.05 (2.07, 20.8%)	12.44 (2.46, 24.6%)	14.11 (4.13, 41.4%)

photosynthesis (Fig. 4) were elevated with septic input. This may be due to local increases in septic water and nutrients increasing ET during the growing season, reducing groundwater recharge, lowering groundwater storage, and reducing watershed baseflow. We also noted that our model tended to underestimate the lowest streamflows during the growing season. Several potential reasons could cause this discrepancy: 1) Higher transpiration estimates caused by uncertainties in vegetation

Hydrology and Earth System Sciences
Discussions

ecophysiological parameters in RHESSys controlling vegetation water use or phenology; 2) Underestimation of groundwater recharge and release to streams during the growing season; and 3) A lack of human modulation of groundwater use during dry periods. During our prior surveys (Law et al., 2004; Fraser et al., 2013) residents stated they had reduced their water use during droughts. While the model underestimation was negligible, additional empirical data about water flux, groundwater processes, and household water management are needed for calibration of RHESSys parameters and would enhance model prediction accuracy of hydrological processes, especially during growing season.

4.2 Nitrogen concentrations and loads

Activating fertilization and septic modules in RHESSys improved the simulations of in-stream NO_3^- concentration and load dynamics compared to the original RHESSys model. Compared to the weekly BES observations, our model underestimated the mean in-stream NO_3^- concentration by 0.1 mg NO_3^--N/L (-7%) with stronger variability (Fig. 5). The underestimation of mean concentration could be attributed to uncertainties in N inputs. While we used mean values from previous studies, actual N inputs from fertilization and septic effluents have considerable variations. It is also important to note that BARN used to have extensive agricultural activities which may have resulted in accumulation of legacy N in the groundwater. Spinning up the model for 30 years may be insufficient to account for the export of this N from groundwater, which possibly caused the lower simulated mean NO_3^- concentration compared to BES measurements. Furthermore, we found the model yielded a stronger seasonality of N export, with simulated concentrations with fertilization and septic processes lower during the growing season but spiking right at the end of growing season. Again, uncertainty in RHESSys vegetation parameters and phenology may contribute to these differences, where the sudden ending of the growing season caused quick mobilization of NO_3^- into streams. Also, the lower estimation of streamflow during the growing season could increase residence time and retention, and reduce N export from uplands and groundwater to streams, causing the underestimation of NO_3^- concentration and load in these periods.

The simulated mean NO_3^- concentration from scenario *none* was significantly greater than the observed concentrations at POBR (Table 3) which provide a reference of forest conditions of watersheds in the area. The higher estimated NO_3^- concentrations in BARN could be explained by the land use difference between the two watersheds. Specifically, there are more impervious areas and lawns in the upland of BARN than in POBR which is fully forested (with the exception of a regional gasline cut with herbaceous vegetation), resulting in lower N uptake and higher N concentration (Table 3, None vs. POBR). This result implies that, even in the absence of additional NO_3^- input from human activities, the water quality in urban watersheds is unlikely to fully recover to pre-urbanization levels due to altered hydrology and differences in vegetation.

In addition to improving predictions of in-stream NO_3^- concentration, the simulated denitrification rates in lawns fell in the range of empirically estimated rates at BARN (Suchy et al., 2023) and other areas in Baltimore (Raciti et al., 2011). Among all hot spots, the constructed wetland and sediment accumulation zone at the base of the gully exhibited the highest denitrification rates within the entire watershed, both before and after considering fertilization and septic processes. These rates were comparable to other wetland denitrification measurements: Groffman and Hanson (1997) estimated denitrification rates from 1 to >130 kg N/ha/year at several wetlands in Rhode Island; Poe et al. (2003) reported rates ranging between 19 to 191 kg N/ha/year at a constructed wetland receiving agricultural runoff; Harrison et al. (2011) found rates of 89 and 158kg N/ha/year at two wetlands adjacent to Minebank Run in Baltimore. In BARN, these wetlands were located in low-slope downstream areas and advertently or inadvertently treat runoff originating from roads and upstream households. Unlike lawns which may not maintain high soil moisture levels, these areas remain consistently wet throughout most of the year. These features create ideal conditions for promoting denitrification and effectively retaining N loads that would otherwise be transported to streams. Specifically, these two wetlands covering only 0.09% of the watershed contributed to 0.39% of the total denitrification during the study period. This discovery highlights the significance of strategically selecting locations for water quality improvement projects in future watershed restoration efforts, and assessing the ecosystem services of spontaneously generated features.

4.3 Model improvements

The analyses here highlight several challenges in modeling mixed land use watersheds such as BARN. First, for septic processes, we assumed septic fields of houses located on the southern divide of BARN contribute drainage inside BARN. Given the high N loads produced by septic systems, more detailed survey for their location relative to the drainage system is necessary. Second, our current setup assumed a uniform daily NO_3^- input and wastewater volume of septic effluents for all houses and fixed fertilization amounts for lawns adjusted by application interval (Eq. 1). These parameters could be further adjusted when more observations are available. For fertilization, our model distributed the estimated total fertilization amount uniformly to all lawns in the watershed, at rates modulated by the proportion of lawns fertilized estimated by Law et al. (2004) and Fraser et al. (2013). In reality, fertilization rate and frequency vary significantly in different lawns. Variable space and time patterns of fertilization rates could result in N hot spots that exceed retention capacity relative to variable transport rates. For irrigation, our model applies irrigation close to its maximum (4 mm/day) when water stress is high, but residents may not irrigate their lawns at these rates during drought to conserve groundwater. Current settings of our model could introduce excessive depletion of groundwater during droughts, and lead to underestimation of baseflow and in-stream NO_3^- concentrations. More detailed information about water usage habits and observations of relationships between meteorological factors and groundwater storage are needed to improve simulation of the dynamics of water withdrawal in RHESSys.

4.4 Synthesis of results

Lastly, our study addressed three overarching questions:

1) What are the individual and interacting contributions of different watershed N sources to streamwater N export?

Simulations with solely septic or fertilization inputs increased NO_3^- export by 1.9 and 2.4 kg NO_3^--N/ha/year individually, while including both sources increased export by 4.7 kg NO_3^--N/ha/year, compared to the base scenario's 1.2 kg NO_3^--N/ha/year with only atmospheric deposition.

https://doi.org/10.5194/hess-2023-256
Preprint. Discussion started: 2 November 2023

Hydrology and Earth System Sciences
Open Access
EGU
Discussions

2) *How do the spatially nested patterns of water and N inputs from human activities alter spatial patterns of a set of key ecohydrological processes including N retention, evapotranspiration, soil and groundwater levels and flows?*

Simulation results indicate septic systems using deep groundwater as the water source, transported that water to shallow soils, which resulted in systematic shallow water table increases within upland residential areas and small drops in water table levels in riparian areas of residential subcatchments. Results show how on-site extraction of water could alter the hydrological conditions of both "on-site" locations where septic effluent is directly disposed, as well as in "off-site" locations. These results occur because while the septic effluent is depleted by evapotranspiration, the deeper groundwater that emerges in riparian areas is unaffected. Thus, extraction of water for domestic use lowers riparian water tables even when this water is ultimately discharged back into the environment via a septic system. Likewise, the spatial pattern of denitrification showed increases not only in sites receiving N inputs directly (i.e., lawns and septic drainage fields) but also in "off-site" downstream areas receiving transported NO_3^- from upland zones.

3) *What are the emergent patterns of N cycling and retention, including hot spots at sites receiving direct additional N and downslope, offsite locations receiving transported N?*

In the residential subcatchments of the watershed, riparian zones, constructed and accidental wetlands were found to be hot spots of denitrification. These areas have the combination of subsidized supplies of water and NO_3^-, providing mixing zones with conditions promoting denitrification that are more consistent than fertilized lawn areas with variable soil moisture. Temporal patterns of denitrification were generally climate-driven and highest rates occurred in spring and summer in both hot spots and other areas in the watershed. These results suggest that effective siting of BMPs and a careful assessment of spontaneously existing (accidental) retention zones can be used to achieve environmental goals for developed watersheds, by leveraging naturally occurring and built features providing ecosystem services.

4.5 Conclusions

Our analysis provides important insights into how different sources of N input interact with ecohydrological processes to control N export from exurban watersheds. While atmospheric deposition is ubiquitous, the input of lawn fertilization and irrigation water, and septic effluent volume and N load are concentrated in limited areas of the watershed. These differences cascade through the watershed producing hot spots of N export and retention. Our results strongly support the idea for watershed-scale analysis and planning to address watershed N exports and are particularly relevant in areas such as the Chesapeake Bay that are highly sensitive to N-induced eutrophication. The improved simulations with more complete, spatially nested inputs of water and N highlight the importance of the structured spatial heterogeneity of human impacts to fully understand ecohydrological processes in developed watersheds. Oversimplified model structures and input could introduce significant bias that are inapplicable to formulate future water improvement plans. The spatially distributed inputs and RHESSys model structure may provide a reliable framework to evaluate current coupled water, C and N cycles, but also

https://doi.org/10.5194/hess-2023-256
Preprint. Discussion started: 2 November 2023

Hydrology and Earth System Sciences Discussions
Open Access

understand and predict effectiveness of ecosystem restorations to improve water quality and ecosystem health in developed watersheds.

Acknowledgements

This work was supported by the National Science Foundation Coastal Science, Engineering, and Education for Sustainability Program, Grant No. 1426819, the National Science Foundation Long-Term Ecological Research (LTER) Program, Grant No. 1027188 for the Baltimore Ecosystem Study, and the Department of Energy Integrated Field Laboratory, Grant No. 004278 for the Baltimore Social-Environment Collaborative.

Code and data availability

The RHESSys program used for this study is available on https://github.com/ruoyu93/RHESSysEastCoast. The model outputs and Python code used to analyse and visualize the outputs (in Jupyter Notebook) are posted to a public Zenodo repository at https://doi.org/10.5281/zenodo.10022932 (Zhang et al., 2023). Other files related to the paper can be requested directly from the corresponding author (Ruoyu Zhang).

Author contribution

Conceptualization and main investigation, writing of the first draft, and visualization of this study was conducted by RZ under the supervision of LEB and PMG. PMG, AKS, JMD, and AJG provided water chemistry and biogeochemical data. All authors reviewed and edited the paper.

Competing interests

The contact author has declared that none of the authors has any competing interests.

https://doi.org/10.5194/hess-2023-256
Preprint. Discussion started: 2 November 2023

Hydrology and Earth System Sciences
Open Access
Discussions

References

Abbott, M. B., Bathurst, J. C., Cunge, J. A., Oconnell, P. E., & Rasmussen, J. (1986a). An Introduction to the European Hydrological System - Systeme Hydrologique Europeen, She .1. History and Philosophy of a Physically-Based, Distributed Modeling System. *Journal of Hydrology*, *87*(1-2), 45-59. https://doi.org/10.1016/0022-1694(86)90114-9

Abbott, M. B., Bathurst, J. C., Cunge, J. A., Oconnell, P. E., & Rasmussen, J. (1986b). An Introduction to the European Hydrological System - Systeme Hydrologique Europeen, She .2. Structure of a Physically-Based, Distributed Modeling System. *Journal of Hydrology*, *87*(1-2), 61-77. https://doi.org/10.1016/0022-1694(86)90115-0

Arnold, J. G., Srinivasan, R., Muttiah, R. S., & Williams, J. R. (1998). Large area hydrologic modeling and assessment - Part 1: Model development. *Journal of the American Water Resources Association*, *34*(1), 73-89. https://doi.org/10.1111/j.1752-1688.1998.tb05961.x

Band, L. E., Cadenasso, M. L., Grimmond, C. S., Grove, J. M., & Pickett, S. T. (2005). Heterogeneity in urban ecosystems: patterns and process. *Ecosystem function in heterogeneous landscapes*, 257-278.

Band, L. E., Patterson, P., Nemani, R., & Running, S. W. (1993). Forest Ecosystem Processes at the Watershed Scale - Incorporating Hillslope Hydrology. *Agricultural and Forest Meteorology*, *63*(1-2), 93-126. https://doi.org/10.1016/0168-1923(93)90024-C

Bao, C., Li, L., Shi, Y. N., & Duffy, C. (2017). Understanding watershed hydrogeochemistry: 1. Development of RT-Flux-PIHM. *Water Resources Research*, *53*(3), 2328-2345. https://doi.org/10.1002/2016wr018934

Bernhardt, E. S., Blaszczak, J. R., Ficken, C. D., Fork, M. L., Kaiser, K. E., & Seybold, E. C. (2017). Control Points in Ecosystems: Moving Beyond the Hot Spot Hot Moment Concept. *Ecosystems*, *20*(4), 665-682. https://doi.org/10.1007/s10021-016-0103-y

Campo, J., & Merino, A. (2016). Variations in soil carbon sequestration and their determinants along a precipitation gradient in seasonally dry tropical forest ecosystems. *Global Change Biology*, *22*(5), 1942-1956. https://doi.org/10.1111/gcb.13244

Carrico, A. R., Fraser, J., & Bazuin, J. T. (2013). Green With Envy: Psychological and Social Predictors of Lawn Fertilizer Application. *Environment and Behavior*, *45*(4), 427-454. https://doi.org/10.1177/0013916511434637

Castiblanco, E. S., Groffman, P. M., Duncan, J., Band, L. E., Doheny, E., Fisher, G. T., ... & Suchy, A. K. (2023). Long-term trends in nitrate and chloride in streams in an exurban watershed. *Urban Ecosystems*, 1-14.

Chen, G., Zhu, H. L., & Zhang, Y. (2003). Soil microbial activities and carbon and nitrogen fixation. *Research in Microbiology*, *154*(6), 393-398. https://doi.org/10.1016/S0923-2508(03)00082-2

Cleaves, E. T., Godfrey, A. E., & Bricker, O. P. (1970). Geochemical balance of a small watershed and its geomorphic implications. *Geological Society of America Bulletin*, *81*(10), 3015-3032. https://doi.org/10.1130/0016-7606(1970)81[3015:GBOASW]2.0.CO;2

Crowther, T. W., Todd-Brown, K. E. O., Rowe, C. W., Wieder, W. R., Carey, J. C., Machmuller, M. B., Snoek, B. L., Fang, S., Zhou, G., Allison, S. D., Blair, J. M., Bridgham, S. D., Burton, A. J., Carrillo, Y., Reich, P. B., Clark, J. S., Classen, A. T., Dijkstra, F. A., Elberling, B., . . . Bradford, M. A. (2016). Quantifying global soil carbon losses in response to warming. *Nature*, *540*(7631), 104-+. https://doi.org/10.1038/nature20150

Cui, J. T., Shao, G. C., Yu, S. E., & Cheng, X. (2016). Influence of controlled drainage on the groundwater nitrogen and phosphorus concentration at jointing-booting stage of wheat. *Journal of Chemistry*, *2016*. https://doi.org/10.1155/2016/5280194

Del Grosso, S. J., Mosier, A. R., Parton, W. J., & Ojima, D. S. (2005). DAYCENT model analysis of past and contemporary soil N2O and net greenhouse gas flux for major crops in the USA. *Soil and Tillage Research*, *83*(1), 9-24. https://doi.org/10.1016/j.still.2005.02.007

Fan, Y., Clark, M., Lawrence, D. M., Swenson, S., Band, L. E., Brantley, S. L., Brooks, P. D., Dietrich, W. E., Flores, A., Grant, G., Kirchner, J. W., Mackay, D. S., McDonnell, J. J., Milly, P. C. D., Sullivan, P. L., Tague, C., Ajami, H., Chaney, N., Hartmann, A., . . . Yamazaki, D. (2019). Hillslope Hydrology in Global Change Research and Earth System Modeling. *Water Resources Research*, *55*(2), 1737-1772. https://doi.org/10.1029/2018wr023903

Fraser, J. C., Bazuin, J. T., Band, L. E., & Grove, J. M. (2013). Covenants, cohesion, and community: The effects of neighborhood governance on lawn fertilization. *Landscape and Urban Planning*, *115*, 30-38. https://doi.org/10.1016/j.landurbplan.2013.02.013

Galloway, J. N., Townsend, A. R., Erisman, J. W., Bekunda, M., Cai, Z. C., Freney, J. R., Martinelli, L. A., Seitzinger, S. P., & Sutton, M. A. (2008). Transformation of the nitrogen cycle: Recent trends, questions, and potential solutions. *Science*, *320*(5878), 889-892. https://doi.org/10.1126/science.1136674

Gold, A. J., DeRagon, W. R., Sullivan, W. M., & Lemunyon, J. L. (1990). Nitrate-nitrogen losses to groundwater from rural and suburban land uses. *Journal of soil and water conservation*, *45*(2), 305-310.

Groffman, P.M., Butterbach-Bahl, K., Fulweiler, R.W., Gold, A.J., Morse, J.L., Stander, E.K., Tague, C., Tonitto, C. and Vidon, P., (2009). Challenges to incorporating spatially and temporally explicit phenomena (hotspots and hot moments) in denitrification models. *Biogeochemistry, 93*, 49-77. https://doi.org/10.1007/s10533-008-9277-5

Groffman, P. M., & Hanson, G. C. (1997). Wetland denitrification: influence of site quality and relationships with wetland delineation protocols. *Soil Science Society of America Journal*, *61*(1), 323-329. https://doi.org/10.2136/sssaj1997.03615995006100010047x

Groffman, P. M., Law, N. L., Belt, K. T., Band, L. E., & Fisher, G. T. (2004). Nitrogen fluxes and retention in urban watershed ecosystems. *Ecosystems*, *7*(4), 393-403. https://doi.org/10.1007/s10021-003-0039-x

Groffman, P. M., Matsler, A. M., & Grabowski, Z. J. (2023). How reliable–and (net) beneficial–is the green in green infrastructure. *Agricultural and Resource Economics Review*, 1-12. https://doi.org/10.1017/age.2023.6

Harrison, M. D., Groffman, P. M., Mayer, P. M., Kaushal, S. S., & Newcomer, T. A. (2011). Denitrification in alluvial wetlands in an urban landscape. *Journal of environmental quality*, *40*(2), 634-646. https://doi.org/10.2134/jeq2010.0335

Hidy, D., Barcza, Z., Marjanović, H., Ostrogović Sever, M.Z., Dobor, L., Gelybó, G., Fodor, N., Pintér, K., Churkina, G., Running, S. and Thornton, P. (2016). Terrestrial ecosystem process model Biome-BGCMuSo v4. 0: summary of improvements and new modeling possibilities. *Geoscientific Model Development*, *9*(12), 4405-4437. https://doi.org/10.5194/gmd-9-4405-2016

Hobbie, S. E., Finlay, J. C., Janke, B. D., Nidzgorski, D. A., Millet, D. B., & Baker, L. A. (2017). Contrasting nitrogen and phosphorus budgets in urban watersheds and implications for managing urban water pollution. *Proceedings of the National Academy of Sciences*, *114*(16), 4177-4182. https://doi.org/10.1073/pnas.1618536114

https://doi.org/10.5194/hess-2023-256
Preprint. Discussion started: 2 November 2023

Hydrology and Earth System Sciences Open Access EGU Discussions

Humphrey, C. P., O'Driscoll, M. A., Deal, N. E., Lindbo, D. L., Thieme, S. C., & Zarate-Bermudez, M. A. (2013). Onsite Wastewater System Nitrogen Contributions to Groundwater in Coastal North Carolina. *Journal of Environmental Health*, *76*(5), 16-22.

Jayasooriya, V. M., & Ng, A. W. M. (2014). Tools for Modeling of Stormwater Management and Economics of Green Infrastructure Practices: a Review. *Water Air and Soil Pollution*, *225*(8). https://doi.org/10.1007/s11270-014-2055-1

Koltsida, E., Mamassis, N., & Kallioras, A. (2023). Hydrological modeling using the Soil and Water Assessment Tool in urban and peri-urban environments: the case of Kifisos experimental subbasin (Athens, Greece). *Hydrology and Earth System Sciences*, *27*(4), 917-931. https://doi.org/10.5194/hess-27-917-2023

Law, N., Band, L., & Grove, M. (2004). Nitrogen input from residential lawn care practices in suburban watersheds in Baltimore County, MD. *Journal of Environmental Planning and Management*, *47*(5), 737-755. https://doi.org/10.1080/0964056042000274452

Lawrence, D.M., Fisher, R.A., Koven, C.D., Oleson, K.W., Swenson, S.C., Bonan, G., Collier, N., Ghimire, B., van Kampenhout, L., Kennedy, D. and Kluzek, E., … & Zeng, X. (2019). The Community Land Model version 5: Description of new features, benchmarking, and impact of forcing uncertainty. *Journal of Advances in Modeling Earth Systems*, *11*(12), 4245-4287. https://doi.org/10.1029/2018MS001583

Lee, J. G., Nietch, C. T., & Panguluri, S. (2018). Drainage area characterization for evaluating green infrastructure using the Storm Water Management Model. *Hydrology and Earth System Sciences*, *22*(5), 2615-2635. https://doi.org/10.5194/hess-22-2615-2018

Lin, L., Band, L. E., Vose, J. M., Hwang, T., Miniat, C. F., & Bolstad, P. V. (2019). Ecosystem processes at the watershed scale: Influence of flowpath patterns of canopy ecophysiology on emergent catchment water and carbon cycling. *Ecohydrology*, *12*(5). https://doi.org/10.1002/eco.2093

Lin, L., Webster, J. R., Hwang, T., & Band, L. E. (2015). Effects of lateral nitrate flux and instream processes on dissolved inorganic nitrogen export in a forested catchment: A model sensitivity analysis. *Water Resources Research*, *51*(4), 2680-2695. https://doi.org/10.1002/2014wr015962

Lowe, K. S., Tucholke, M. B., Tomaras, J. M., Conn, K., Hoppe, C., Drewes, J. E., McCray, J. E., & Munakata-Marr, J. (2009). *Influent constituent characteristics of the modern waste stream from single sources*. Water Environment Research Foundation.

Martini, N. F., Nelson, K. C., Hobbie, S. E., & Baker, L. A. (2015). Why "Feed the Lawn"? Exploring the Influences on Residential Turf Grass Fertilization in the Minneapolis-Saint Paul Metropolitan Area. *Environment and Behavior*, *47*(2), 158-183. https://doi.org/10.1177/0013916513492418

Maxwell, R. M. (2013). A terrain-following grid transform and preconditioner for parallel, large-scale, integrated hydrologic modeling. *Advances in Water Resources*, *53*, 109-117. https://doi.org/10.1016/j.advwatres.2012.10.001

McClain, M. E., Boyer, E. W., Dent, C. L., Gergel, S. E., Grimm, N. B., Groffman, P. M., Hart, S. C., Harvey, J. W., Johnston, C. A., Mayorga, E., McDowell, W. H., & Pinay, G. (2003). Biogeochemical hot spots and hot moments at the interface of terrestrial and aquatic ecosystems. *Ecosystems*, *6*(4), 301-312. https://doi.org/10.1007/s10021-003-0161-9

Nash, J. E., & Sutcliffe, J. V. (1970). River flow forecasting through conceptual models part I—A discussion of principles. *Journal of Hydrology*, *10*(3), 282-290. https://doi.org/10.1016/0022-1694(70)90255-6

Nobre, A. D., Cuartas, L. A., Hodnett, M., Renno, C. D., Rodrigues, G., Silveira, A., Waterloo, M., & Saleska, S. (2011). Height Above the Nearest Drainage - a hydrologically relevant new terrain model. *Journal of Hydrology*, *404*(1-2), 13-29. https://doi.org/10.1016/j.jhydrol.2011.03.051

Oleson, K. W., Niu, G. Y., Yang, Z. L., Lawrence, D. M., Thornton, P. E., Lawrence, P. J., Stockli, R., Dickinson, R. E., Bonan, G. B., Levis, S., Dai, A., & Qian, T. (2008). Improvements to the Community Land Model and their impact on the hydrological cycle. *Journal of Geophysical Research-Biogeosciences*, *113*(G1). https://doi.org/10.1029/2007jg000563

Palta, M. M., Grimm, N. B., & Groffman, P. M. (2017). "Accidental" urban wetlands: ecosystem functions in unexpected places. *Frontiers in Ecology and the Environment*, *15*(5), 248-256. https://doi.org/10.1002/fee.1494

Parton, W. J., Mosier, A. R., Ojima, D. S., Valentine, D. W., Schimel, D. S., Weier, K., & Kulmala, A. E. (1996). Generalized model for N2 and N2O production from nitrification and denitrification. *Global biogeochemical cycles*, *10*(3), 401-412. https://doi.org/10.1029/96gb01455

Pastor, J., & Post, W. M. (1986). Influence of Climate, Soil-Moisture, and Succession on Forest Carbon and Nitrogen Cycles. *Biogeochemistry*, *2*(1), 3-27. https://doi.org/10.1007/Bf02186962

Poe, A. C., Piehler, M. F., Thompson, S. P., & Paerl, H. W. (2003). Denitrification in a constructed wetland receiving agricultural runoff. *Wetlands*, *23*(4), 817-826. http://doi.org/10.1672/0277-5212(2003)023[0817:DIACWR]2.0.CO;2

Putnam, S. M. (2018). The influence of landscape structure on storage and streamflow generation in a piedmont catchment (Doctoral dissertation, Johns Hopkins University).

Rossman, L. A. (2010a). Modeling Low Impact Development Alternatives with SWMM. *Journal of Water Management Modeling*, 167-182. https://doi.org/10.14796/Jwmm.R236-11

Rossman, L. A. (2010b). *Storm water management model user's manual, version 5.0*. U.S. Environmental Protection Agency.

Running, S. W., & Coughlan, J. C. (1988). A General-Model of Forest Ecosystem Processes for Regional Applications .1. Hydrologic Balance, Canopy Gas-Exchange and Primary Production Processes. *Ecological Modelling*, *42*(2), 125-154. https://doi.org/10.1016/0304-3800(88)90112-3

Running, S. W., & Gower, S. T. (1991). Forest-Bgc, a General-Model of Forest Ecosystem Processes for Regional Applications .2. Dynamic Carbon Allocation and Nitrogen Budgets. *Tree Physiology*, *9*(1-2), 147-160. https://doi.org/10.1093/treephys/9.1-2.147

Running, S. W., & Hunt, E. R. (1993). Generalization of a Forest Ecosystem Process Model for Other Biomes, BIOME-BGC, and an Application for Global-Scale Models. In J. R. Ehleringer & C. B. Field (Eds.), *Scaling Physiological Processes* (pp. 141-158). Academic Press. https://doi.org/10.1016/B978-0-12-233440-5.50014-2

Samimi, M., Mirchi, A., Moriasi, D., Ahn, S., Alian, S., Taghvaeian, S., & Sheng, Z. P. (2020). Modeling arid/semi-arid irrigated agricultural watersheds with SWAT: Applications, challenges, and solution strategies. *Journal of Hydrology*, *590*. https://doi.org/10.1016/j.jhydrol.2020.125418

St. Clair, J., Moon, S., Holbrook, W.S., Perron, J.T., Riebe, C.S., Martel, S.J., Carr, B., Harman, C., Singha, K.D. and Richter, D.D., (2015). Geophysical imaging reveals topographic stress control of bedrock weathering. *Science*, *350*(6260), 534-538. https://doi.org/10.1126/science.aab2210

Suchy, A. K., Groffman, P. M., Band, L. E., Duncan, J. M., Gold, A. J., Grove, J. M., Locke, D. H., Templeton, L., & Zhang, R. (2023). Spatial and Temporal Patterns of Nitrogen Mobilization in Residential Lawns. *Ecosystems*. https://doi.org/10.1007/s10021-023-00848-y

Tague, C. L., & Band, L. E. (2004). RHESSys: Regional Hydro-Ecologic Simulation System-An Object-Oriented Approach to Spatially Distributed Modeling of Carbon, Water, and Nutrient Cycling. *Earth Interactions*, *8*. https://doi.org/10.1175/1087-3562(2004)8<1:RRHSSO>2.0.CO;2

Wang, G. S., Huang, W. J., Zhou, G. Y., Mayes, M. A., & Zhou, J. Z. (2020). Modeling the processes of soil moisture in regulating microbial and carbon-nitrogen cycling. *Journal of Hydrology*, *585*. https://doi.org/10.1016/j.jhydrol.2020.124777

Zhang, R. (2023). RHESSys model and outputs for Baisman Run [Data set]. Zenodo. https://doi.org/10.5281/zenodo.10034198

Zhi, W., Shi, Y. N., Wen, H., Saberi, L., Ng, G. H. C., Sadayappan, K., Kerins, D., Stewart, B., & Li, L. (2022). BioRT-Flux-PIHM v1.0: a biogeochemical reactive transport model at the watershed scale. *Geoscientific Model Development*, *15*(1), 315-333. https://doi.org/10.5194/gmd-15-315-2022